Earth and Space Science

RESEARCH ARTICLE
10.1029/2025EA004590

Special Collection:
The Lunar Trailblazer Mission Collection: Mission, Instruments, Data Analysis Plan

Mid-Infrared Compositional Spectral Parameters for the Lunar Thermal Mapper Instrument Onboard Lunar Trailblazer

Katherine A. Shirley[1], Kerri L. Donaldson Hanna[2], Neil E. Bowles[1], Namrah Habib[1], Nicholas Elkington[1], Rory Evans[1], Christopher S. Edwards[3], Tristram Warren[1], Fiona Henderson[1], Christopher Haberle[3], Rachel L. Klima[4], and Bethany L. Ehlmann[5]

[1]Atmospheric Oceanic and Planetary Physics Department, University of Oxford, Oxford, UK, [2]Department of Physics, University of Central Florida, Orlando, FL, USA, [3]Northern Arizona University, Flagstaff, AZ, USA, [4]Johns Hopkins Applied Physics Laboratory, Laurel, MD, USA, [5]Division of Geological & Planetary Sciences, California Institute of Technology, Pasadena, CA, USA

Abstract The Lunar Trailblazer mission launched in February of 2025 with the goal of characterizing lunar surface water through a targeted campaign. One instrument on the mission, the Lunar Thermal Mapper (LTM), was tasked with measuring the surface temperature to compare with maps of the form and abundance of water on the lunar surface. LTM's secondary science goals were to identify regolith composition and thermophysical properties as exhibited by mid-infrared spectral features. Here we show the utility of LTM in distinguishing lunar regolith composition with its 11 narrow bands. Five spectral parameter products were developed to aid in early identification of regions of interest for follow-on spectral analyses. These products include the Christiansen feature (CF) value, weighted absorption center (WAC) value, WAC band depth, Transparency Roll-off, and a Diviner CF value equivalent. These products would be used mainly to flag these regions for more detailed follow-up study with the entire spectral capabilities of the mission instrumentation.

Plain Language Summary The Lunar Thermal Mapper (LTM) is one of two instruments on the Lunar Trailblazer mission launched in February 2025. LTM's primary goal is to provide surface temperature measurements for the lunar surface, in particular for identifying and mapping water on the Moon. LTM is also capable of identifying the compositional and physical properties of different rocks on the surface. Here, we test those capabilities and determine five methods for quickly distinguishing bulk properties of the lunar rocks that can be used by the community to identify regions of interest for further investigation.

Key Points:

- Mid-infrared compositional parameters were created and tested for the Lunar Trailblazer mission
- Spectral parameters can distinguish bulk silicate mineralogy, and identify regions of compositional interest
- The Christiansen feature roll-off parameter can provide an initial identification of areas with distinct thermophysical properties

Supporting Information:

Supporting Information may be found in the online version of this article.

Correspondence to:

K. A. Shirley,
katherine.shirley@physics.ox.ac.uk

Citation:

Shirley, K. A., Donaldson Hanna, K. L., Bowles, N. E., Habib, N., Elkington, N., Evans, R., et al. (2026). Mid-infrared compositional spectral parameters for the Lunar Thermal Mapper instrument onboard Lunar Trailblazer. *Earth and Space Science*, *13*, e2025EA004590. https://doi.org/10.1029/2025EA004590

Received 11 JUL 2025
Accepted 7 MAR 2026

Author Contributions:

Conceptualization: Katherine A. Shirley, Kerri L. Donaldson Hanna, Neil E. Bowles, Rory Evans, Tristram Warren, Christopher Haberle, Rachel L. Klima, Bethany L. Ehlmann
Formal analysis: Katherine A. Shirley
Funding acquisition: Neil E. Bowles, Bethany L. Ehlmann
Investigation: Katherine A. Shirley, Kerri L. Donaldson Hanna

1. Introduction

The primary goal of the Lunar Trailblazer mission is to characterize lunar surface water through a targeted mapping campaign (Ehlmann et al., 2026). The mission scientific payload consists of two instruments: the High-resolution Volatiles and Minerals Moon Mapper (HVM^3) (Thompson et al., 2025) and the Lunar Thermal Mapper (LTM) (Bowles et al., 2026), which will measure the surface in tandem to create higher spatial and spectral resolution infrared data sets than any previous instrumentation in orbit around the Moon. The mission aims to answer outstanding questions about the form, abundance, and distribution of water on the Moon and the lunar water cycle. Mission objectives are to (a) detect and map water on the lunar surface at key targets to determine its form (OH, H_2O, or ice), abundance, and distribution as a function of latitude, regolith maturity, and lithology; (b) assess possible time-variations in lunar water on sunlit surfaces; and (c) map the form, abundance, and distribution of water ice in the permanently shadowed regions to identify any operationally useful deposits of lunar water and locations where it is exposed at the surface for sampling; and (d) measure surface temperature to quantify the local gradients and search for small cold traps (Ehlmann et al., 2022, 2026).

While the primary goals for the mission are dedicated to understanding lunar water, the data will also provide greater insights into key science and exploration questions about the mineralogy, thermophysical properties, and geologic history of the lunar surface. Here, we focus on the ways in which we can use the LTM to examine the lunar surface and the primary compositional parameters defined for the mid-infrared that will be employed to quickly characterize the targeted regions. These parameters will enable us to identify areas of interest within the targeted regions to then further investigate with the full scope of spectral capabilities of the mission.

Methodology: Katherine A. Shirley, Kerri L. Donaldson Hanna, Neil E. Bowles, Namrah Habib, Nicholas Elkington, Rory Evans, Christopher S. Edwards, Tristram Warren
Project administration: Bethany L. Ehlmann
Resources: Katherine A. Shirley, Kerri L. Donaldson Hanna, Nicholas Elkington, Christopher S. Edwards, Christopher Haberle, Rachel L. Klima, Bethany L. Ehlmann
Software: Namrah Habib, Nicholas Elkington, Rory Evans, Tristram Warren
Validation: Namrah Habib, Bethany L. Ehlmann
Writing – original draft: Katherine A. Shirley
Writing – review & editing: Kerri L. Donaldson Hanna, Neil E. Bowles, Namrah Habib, Fiona Henderson, Rachel L. Klima, Bethany L. Ehlmann

1.1. The Lunar Thermal Mapper: Instrument Overview

A detailed description of the LTM instrument design and performance can be found in Bowles et al. (2026). Briefly, LTM is a spectral radiometer with 15 filters: four broadband filters covering 6–100 μm will constrain lunar surface temperature, while 11 narrowband filters covering 6–10 μm will investigate composition (Table 1) at a ∼70 m/pixel resolution. LTM's primary purpose is to acquire maps of temperatures of the lunar surface at the same time as maps of the form and abundance of water are acquired in order to understand the degree to which temperature controls water on the Moon's surface. However, the narrowband channels, which are the focus of this paper, will allow further investigation of lunar surface compositional and thermophysical properties. Following the lead of the Diviner Lunar Radiometer Experiment (Diviner; Paige et al., 2010), LTM will capture key compositionally diagnostic features to determine mineralogy and thus constrain rock types and lithologies. While Diviner's compositional products are limited to mapping the Christiansen feature (CF) across the lunar surface, LTM's increased spectral coverage (Figure 1) will allow us to explore additional spectral features within the thermal infrared (TIR; ∼6–25 μm).

1.2. Compositional Spectral Features in the Thermal Infrared

The thermal infrared contains a host of spectral features useful in determining bulk mineralogy. LTM will be able to capture more spectral information with its 11 narrow band filters than any previous thermal infrared instrument sent to the Moon. These features include the CF, reststrahlen bands (RB), and transparency features (TF).

The CF is an emissivity maximum that occurs near the Christiansen frequency where the real refractive index of the material is approximately equal to the refractive index of the medium ($n = 1$ for air or vacuum) and where the imaginary refractive index, k, is small. Its wavelength position is indicative of silica polymerization where highly polymerized (framework) silicates have a CF at shorter wavelengths/higher wavenumbers and isolated silica tetrahedra have longer wavelength/lower wavenumbers CFs (Conel, 1969; Logan et al., 1973). The RBs are emissivity minima (reflectance maxima) caused by the stretching and bending of bonds between silicon, oxygen and various cations, and are therefore important in identifying feldspars, pyroxenes, and olivine, among other minerals (e.g., Conel, 1969; Donaldson Hanna et al., 2012; Hamilton & Christensen, 2000; Lyon, 1964). The TFs are emissivity minima caused by volume scattering and become more pronounced as particle size decreases (e.g., Cooper et al., 2002; Hunt & Vincent, 1968; Mustard & Hays, 1997; Salisbury & Eastes, 1985; Salisbury & Wald, 1992; Salisbury et al., 1987; Shirley & Glotch, 2019).

Previous studies (e.g., Hamilton & Christensen, 2000; Hunt & Vincent, 1968; Lyon, 1964; Mustard & Hays, 1997; Salisbury & Eastes, 1985; Salisbury & Wald, 1992; Salisbury et al., 1987; Shirley & Glotch, 2019) have shown the importance of particle size on both the RBs, which lose spectral contrast, and TFs, which gain spectral contrast, as particle size decreases when measured under ambient conditions. Studies performed under lunar environment conditions, that is, under vacuum and heated to lunar surface temperatures, (e.g., Conel, 1969; Donaldson Hanna et al., 2012; Henderson & Jakosky, 1994; Salisbury et al., 1970; Shirley & Glotch, 2019) have shown shifts in the CF position, RB contrast, and TF contrast compared to spectra of the same sample measured under ambient conditions. These changes are due to the environment conditions and some occur as a function of particle size of the sample. Notably, they have observed an inverted correlation between RB spectral contrast and particle size compared to that observed under terrestrial conditions, while TF contrast appears to maintain the trend of increasing with decreasing particle size. Brown (2023) demonstrated that the TF region at shorter wavelengths than the CF (see Figure 1) provides a broad feature that correlates strongly with the particle size of the sample, largely for particulates of <100 μm.

While LTM is at lower spectral resolution compared to laboratory spectrometers, its 11 narrow band channels will cover a range that encompasses at least one of each of these features depending on the mineral (Figure 2). The goal of this investigation is therefore to analyze how well these features can be determined with the LTM resolution using several laboratory spectral data sets down-sampled to LTM resolution and to develop optimized mid-infrared spectral parameters for flagging and mapping compositional or physical properties variation in LTM data.

Table 1
Locations of Lunar Thermal Mapper Narrowband Filter Centers in Wavelength and Wavenumber as Compared to Diviner

LTM narrowband filter centers		
(±20 cm^{-1})	(μm)	Diviner narrowband filters
1,429	7.00 ± 0.20	
1,379	7.25 ± 0.21	
1,333	7.50 ± 0.23	
1,290	7.75 ± 0.24	7.8 ± 0.25
1,250	8.00 ± 0.26	
1,212	8.25 ± 0.27	8.2 ± 0.22
1,176	8.50 ± 0.29	8.5 ± 0.20
1,143	8.75 ± 0.31	
1,111	9.00 ± 0.32	
1,053	9.50 ± 0.36	
1,000	10.00 ± 0.40	

Note. LTM filter widths are ~40 cm^{-1}, as are Diviner filters at 1,212 and 1,176 cm^{-1}, but the Diviner 1,290 cm^{-1} filter is ~80 cm^{-1} wide.

2. Data and Methods

All data and methods were processed and tested using Matlab licensed software, using built-in functions and custom code.

2.1. Data

This research uses several laboratory emissivity data sets measured under both ambient and simulated lunar environment conditions by LTM team members Donaldson Hanna and Shirley (Donaldson Hanna et al., 2017; Glotch et al., 2017; Shirley & Glotch, 2019). These include 10 Apollo bulk regolith samples, 8 silicate minerals, and 8 terrestrial volcanic samples (Table 2), all of which are published data sets aside from several USGS volcanic samples measured under ambient conditions following the procedures outlined in Donaldson Hanna et al. (2021) for this work (see Availability Statement). These samples were chosen to investigate the majority of materials likely to be measured: regolith (Apollo samples); a series of silicate minerals which have been identified in lunar regolith and which have widely distinct spectroscopic features; and terrestrial volcanic whole rock samples that represent lithologies likely to be found on the Moon, ranging from the basalts to the more felsic volcanic material identified at silicic domes (Glotch et al., 2010). The 8 mineral samples and 3 of the volcanic samples are split into particle size fractions. By using these particle size dependent spectral data sets, we can also investigate the influence a physical property variable on the spectra and the ability to distinguish a thermophysical property from the LTM data. As correlation between particle size and the TF roll-off region has been demonstrated (Brown, 2023), this was the only parameter tested using the multi-size binned data. For all other parameters, only the 32–63 μm particle size was used to compare to the other samples.

We use the measured filter response from both Diviner and LTM to down-sample the laboratory data to instrument resolution (Bowles et al., 2026; Paige et al., 2010). Plots of the laboratory spectra and LTM down-sampled spectra are plotted in Figure 2.

2.2. Methods

2.2.1. Christiansen Feature Determination

The main compositional data product for LTM is the CF value parameter for general compositional identification and as a comparison to the previous thermal instrument Diviner. The CF value was derived from Diviner data by performing a quadratic fit across its three compositional filters (Table 1), then using the wavelength where the maximum emissivity is identified as the Diviner CF value (Greenhagen et al., 2010). However, this approach is less straightforward with the increased spectral complexity captured by LTM's 11 channels (e.g., Figure 2).

To optimize the methodology for determining the LTM CF value, we tested several fitting methods:

1. Full curve fit: As a first step, this method fits a third degree polynomial to the entire 11 channel spectrum, then uses the maximum critical point as the CF value.
2. Diviner-like fit: This method fits a quadratic to the three LTM channels that overlap with Diviner at 7.75, 8.25, and 8.5 μm. The wavelength of the maximum emissivity of that fit is then used as the CF value.
3. Moving window fit: This method builds on the "Diviner-like" fit to account for compositions with CF values outside of the 7.75–8.5 μm range. We use the CF value determined from method 2, unless it cannot be determined due to poor fit or the maximum lies outside the range. For those cases, we then use the slope index (Glotch et al., 2010) to determine the likely direction (shorter or longer wavelength) of the maximum. The parabolic fitting window is then shifted to 7.0–7.75 μm for shorter wavelength CFs and 8.5–9.5 μm for longer wavelength CFs, and a new fit and maximum are found.
4. Max value fit: The final method locates the channel with the maximum emissivity value (C_{max}), then fits a third degree polynomial to C_{max} ± 2 channels. The wavelength of the maximum of the fit is then taken as the CF value. A cubic fit rather than a parabolic fit was chosen to better account for the asymmetrical nature of the CF feature in many emissivity spectra.

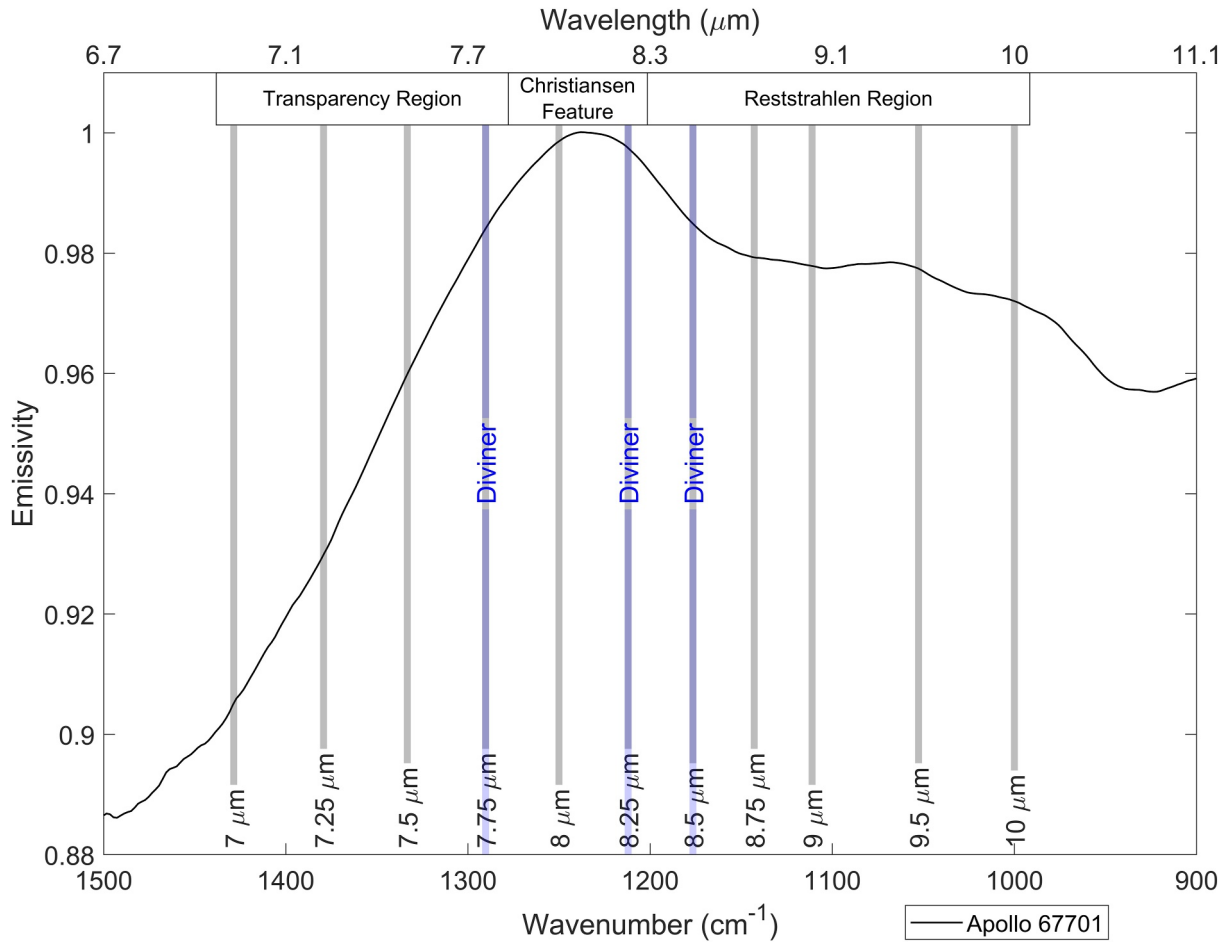

Figure 1. Example laboratory spectrum of Apollo bulk regolith sample 67701 overlain by the center positions for the 11 Lunar Thermal Mapper narrow filters, the centers for the 3 Diviner filters, and the investigated regions of interest for spectral classification. Note that the spectral feature regions shown are for this sample, and while they are generally within these wavelength ranges, the exact wavelength range and emissivity intensity will shift with composition and thermophysical properties.

2.2.2. Transparency Region Characterization

There is a TF region of the electromagnetic spectrum at wavelengths just short of the CF for most minerals, that has been shown to correlate with particle size (e.g., Brown, 2023; Ruff & Christensen, 2002). This "roll-off" parameter will capture the slope of the emissivity short of the determined CF value. To determine the utility of this parameter and best determination, we investigated two methods:

1. Calculated CF to channel 1 slope: This method determines the slope between the 7.0-μm channel and the calculated CF value (both emissivity and wavelength) from the above fitting.
2. True max value to channel 1 slope: This method determines the slope between the 7.0-μm channel and the measured maximum (the emissivity and wavelength of C_{max}).

2.2.3. Reststrahlen Band Characterization

The RBs require detailed investigation for useful compositional analysis, but as first-order metrics, we investigate methods to classify the region longward of the CF value in terms of the wavelength position of the minimum emissivity value and band depth.

2.2.3.1. RB Value

Because RBs are determined by chemistry and structure of the investigated material, there are often several emissivity minima in the region longward of the CF that give us information about the mineral constituents.

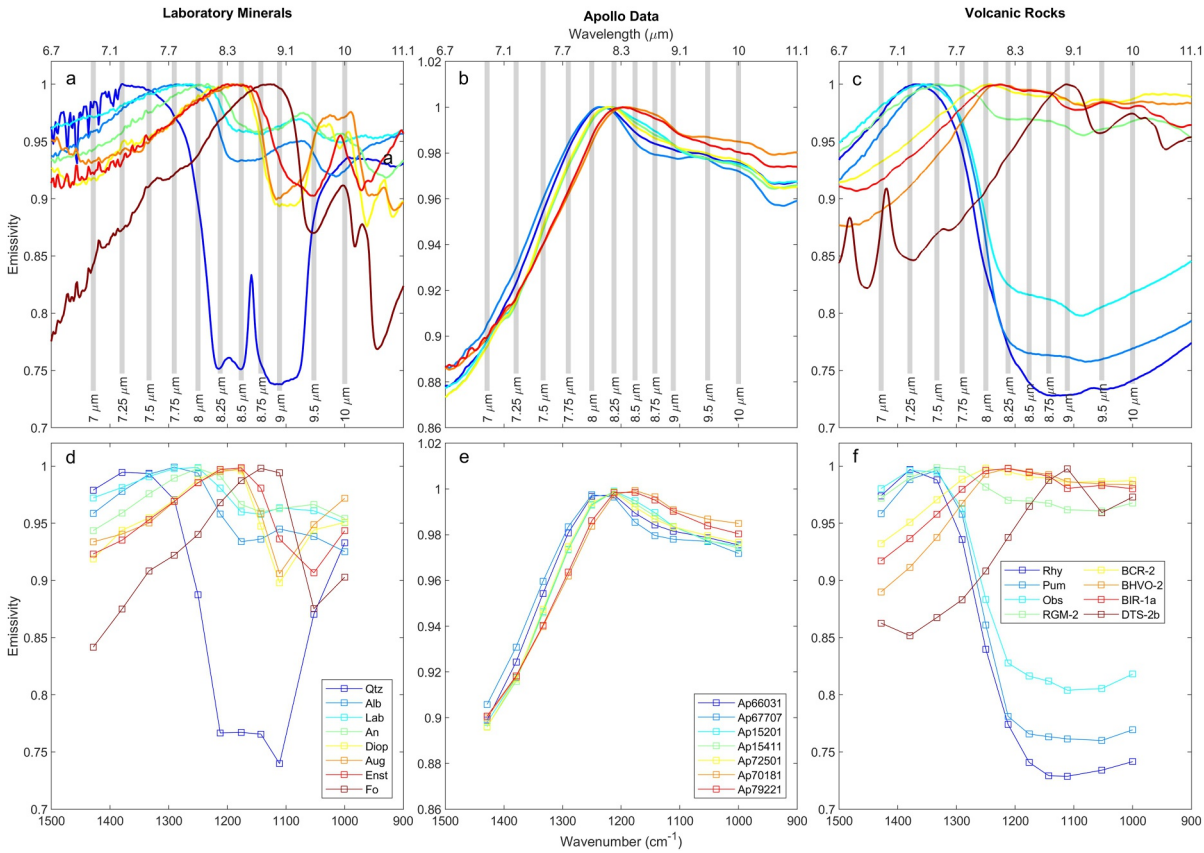

Figure 2. The spectra used in this study split into laboratory resolution emissivity spectra of minerals (a), Apollo samples (b), and volcanic rocks (c) overlain with the position of the Lunar Thermal Mapper (LTM) filters, and their down-sampled (LTM resolution) spectra (d–f, respectively). Full names and descriptions of the samples are provided in Table 2.

However, for more mafic materials, like pyroxene and olivine, that have longer CF values, this can mean that their RBs are not well captured by LTM's spectral coverage. Therefore, we put heavy caveats on this parameter as it may not actually capture the whole RB feature but will give an average minimal point within the region. We have looked at two options to determine an RB position:

1. Simply using the minimum of the emissivity spectrum longward of the determined CF value.
2. Using a weighted absorption center (WAC) approach. The determination of the LTM WAC is based on the methods described in Amador and Bandfield (2016), Smith et al. (2013), and Vincent and Thomson (1972). We limit the LTM spectrum to all values longward of the CF value, interpolate the spectrum to give more data points using a spline function, then integrate over the region to determine a minimum using Equation 1 (adapted from Smith et al. (2013)):

$$\int_{\lambda_{\min}}^{\lambda_c} (1-\varepsilon)\delta\lambda = 0.5\int_{\lambda_{\min}}^{\lambda_{\max}} (1-\varepsilon)\delta\lambda \quad (1)$$

where λ_c is defined as the WAC wavelength, $\lambda_{\min}$ and $\lambda_{\max}$ are the minimum and maximum wavelengths and ε is emissivity.

2.2.3.2. RB Band Depth

Band depth is a common and useful spectral parameter used to investigate the "strength" of a feature. Particularly in lunar regolith, the band depth is an indicator of the thermophysical properties of the surface and influenced by factors such as space weathering, composition and particle size. We determine a band depth from both above methods by taking 1-$\varepsilon_{RB,}$ where ε_{RB} is the emissivity value at the determined RB wavelength.

Table 2
Laboratory Sample Spectra Used in This Investigation

Sample	Shorthand	Source/Reference	Particulate size(s)
Mineral Samples			
Quartz	qtz	Shirley and Glotch (2019)	<32, 32–63, 63–90, 90–125, 125–250, >250 μm
Albite	alb	Shirley and Glotch (2019)	<32, 32–63, 63–90, 90–125, 125–250, >250 μm
Labradorite	lab	Shirley and Glotch (2019)	<32, 32–63, 63–90, 90–125, 125–250, >250 μm
Anorthite	an	Shirley and Glotch (2019)	<32, 32–63, 63–90, 90–125, 125–250, >250 μm
Diopside	diop	Shirley and Glotch (2019)	<32, 32–63, 63–90, 90–125, 125–250, >250 μm
Augite	aug	Shirley and Glotch (2019)	<32, 32–63, 63–90, 90–125, 125–250, >250 μm
Enstatite	enst	Shirley and Glotch (2019)	<32, 32–63, 63–90, 90–125, 125–250, >250 μm
Forsterite	fo	Shirley and Glotch (2019)	<32, 32–63, 63–90, 90–125, 125–250, >250 μm
Apollo Samples			
67701	ap67701	Donaldson Hanna et al. (2017)	<1 mm
66031	ap66031	Donaldson Hanna et al. (2017)	<1 mm
14259	ap14259	Donaldson Hanna et al. (2017)	<1 mm
15201	ap15201	Donaldson Hanna et al. (2017)	<1 mm
15411	ap15411	Donaldson Hanna et al. (2017)	<1 mm
72501	ap72501	Donaldson Hanna et al. (2017)	<1 mm
15071	ap15071	Donaldson Hanna et al. (2017)	<1 mm
70181	ap70181	Donaldson Hanna et al. (2017)	<1 mm
79221	ap79221	Donaldson Hanna et al. (2017)	<1 mm
10084	ap10084	Donaldson Hanna et al. (2017)	<1 mm
Rock samples			
Rhyolite	rhy	Glotch et al. (2017)	<32, 32–63, 63–90, 90–125, 125–180,180–250 μm
Pumice	pum	Glotch et al. (2017)	<32, 32–63, 63–90, 90–125, 125–180,180–250 μm
Obsidian	obs	Glotch et al. (2017)	<32, 32–63, 63–90, 90–125, 125–180,180–250 μm
Dunite	DTS-2b	USGS—Twin Sisters	<45 μm
Basalt	BIR-1a	USGS—Iceland	<45 μm
Basalt	BHVO-2	USGS—Hawaii	<45 μm
Basalt	BCR-2	USGS—Columbia River	<45 μm
Rhyolite	RGM-2	USGS—Glass Mountain	<45 μm

Note. USGS samples are measured at U. Oxford Planetary Spectroscopy Facility following methods of Donaldson Hanna et al. (2021).

3. Results

3.1. Christiansen Feature

The utility of the CF fitting techniques that we examined was dependent on the sample composition. A summary of the calculated LTM CF values as compared to the laboratory resolution spectra is shown in Figure 3 (data values in Table S1 in Supporting Information S1). Fitting the entire 11-point LTM resolution spectrum (LTM poly fit, squares in Figure 3) consistently gave CF values near the middle of the LTM spectral range (~8.5 μm), generally at longer wavelengths than the true CF value. The poor performance of this method can be seen in terms of root-mean-square error (RMSE; Table 3). The Diviner fit (RMSE ~ 100 cm^{-1}) does well within the Diviner wavelength range, but outside of that range, particularly where the CF value <8 μm, it does not perform well, with CF values off by ~300 cm^{-1} or ~2 μm. Both the moving window and max-value fits performed relatively well (RMSE of 25 and 9 cm^{-1}, respectively), with the max-value fit most consistently determining the CF value closest

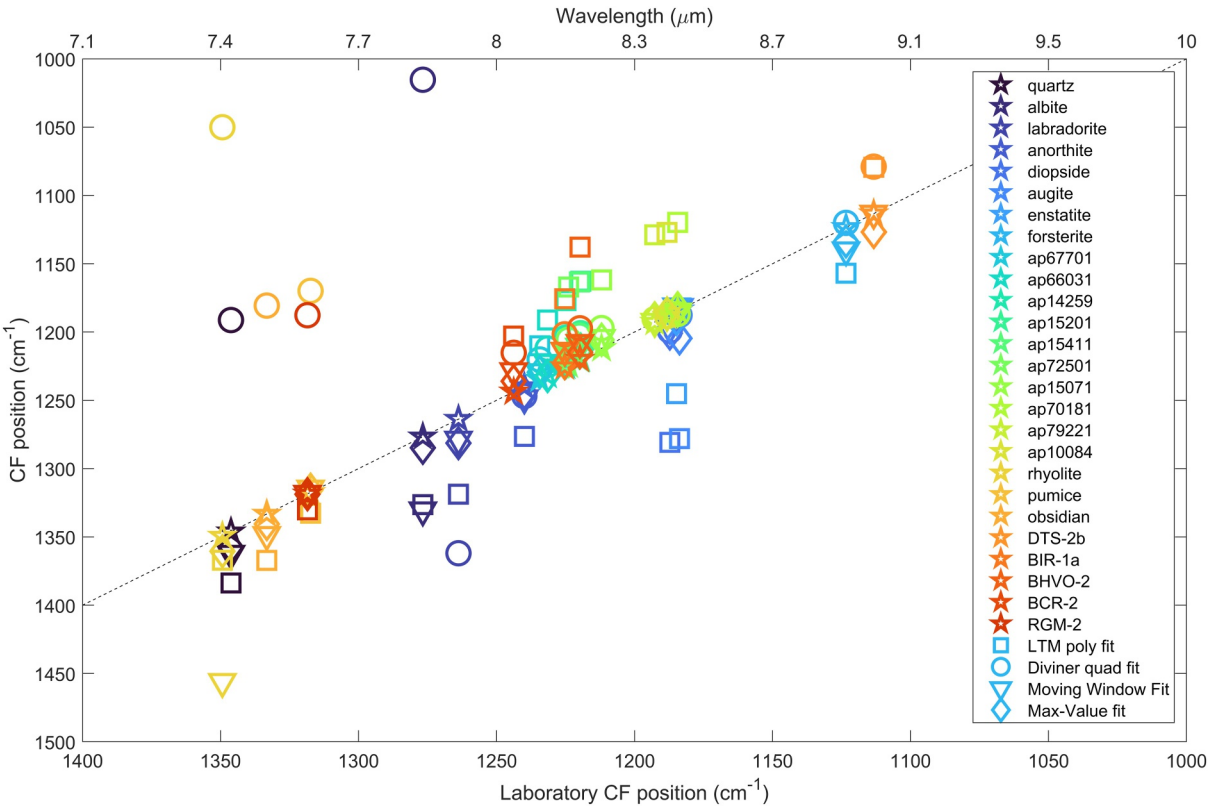

Figure 3. Comparison of Christiansen feature (CF) value determined by different fitting techniques (represented by different symbols) compared to the CF value determined from the laboratory resolution test spectra (stars). All data shown here are measured under ambient conditions and using the 32–63 μm particle size for samples with multiple particle size bins. Exact values are shown in Table S1 in Supporting Information S1.

to the true laboratory derived value. This method also has fewer steps to the CF determination, making it easier to implement.

3.2. Transparency Region

Changes in TF slope were tested on the samples for which we have multiple particle size fractions: the minerals, and the rhyolite, obsidian, and pumice samples. The TF slope was calculated using the two proposed methods and compared per sample. The results were similar for all samples, and as an example, Figure 4 shows the spectra and derived slope/roll-off values for the rhyolite sample. Generally, the slope shortward of the CF position increases with decreasing particle size and the two methods used to calculate the LTM TF slope both reflect this trend. Figure 4b shows the accuracy of the methods compared to the laboratory resolution data, with the "calculated CF" method (Section 2.2.2 Method 1) providing values closer to true.

Table 3
Root-Mean-Squared Error for the Christiansen Feature Fitting Methods in Wavenumber (cm^{-1}) for the Ambient Data Shown in Figure 3 and Table S1 in Supporting Information S1

Method	RMSE (cm^{-1})
LTM poly fit	53.05
Diviner quad fit	99.85
Moving window fit	25.23
Max value fit	8.58

3.3. Reststrahlen Band Region

A comparison of the calculated LTM RB position to the derived position of the first RB minimum per sample spectrum is shown in Figure 5 for our full spectral library. Neither method is accurate, and both overestimate (longer wavelength/shorter wavenumber) the RB position in many cases (Figure 5; values in Table S2 in Supporting Information S1). The inaccuracy was predictable, as the LTM spectral range does not always capture the full RB region, nor even the first RB minimum. However, the LTM WAC approach (RMSE ~40 cm^{-1}) is better at giving a variation in the parameter, allowing at least a qualitative assessment of the material/terrain composition. In contrast, the "minimum" method (RMSE ~78 cm^{-1}) returns, by construction, discrete

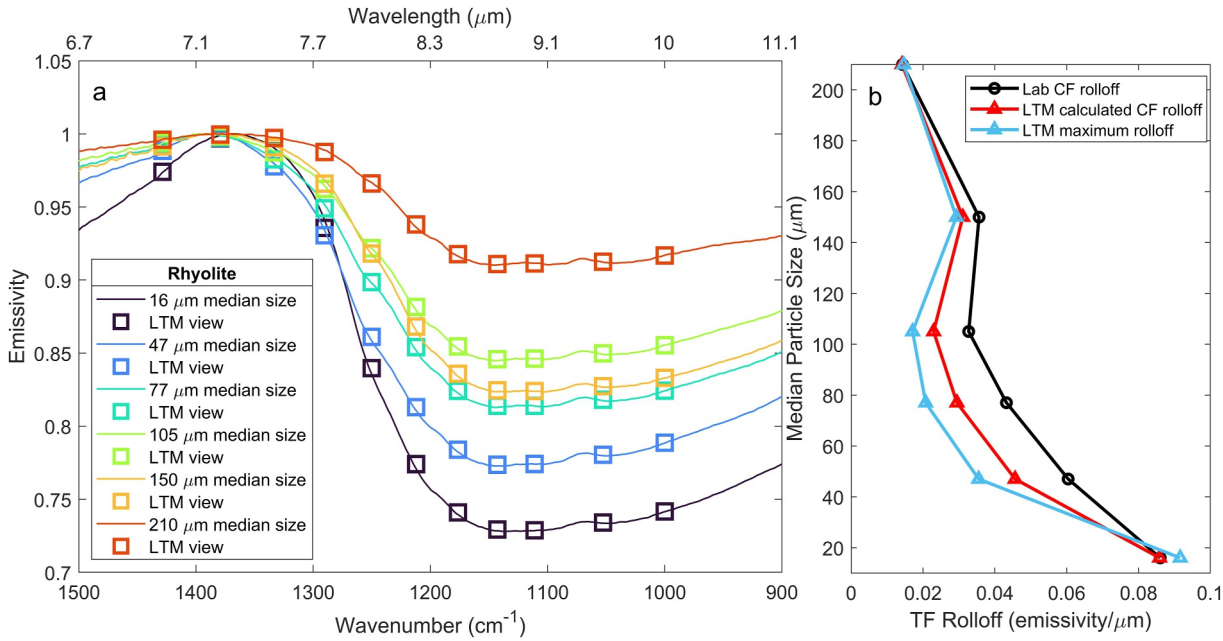

Figure 4. The laboratory resolution and Lunar Thermal Mapper resolution spectra (a) and comparison of methods for transparency features roll-off/slope with median particle size (b) of rhyolite sample.

values corresponding to the spectral positions of the LTM filters; as a consequence, materials with very distinct compositions can be assigned the same value, and often the minimum value is at the 10 μm filter.

4. Discussion

4.1. Christiansen Feature

The LTM CF value will provide a rapid first-order assessment of the bulk composition of a region and LTM's improved coverage of the TIR will distinguish more "extreme" compositions than was possible with Diviner. While Diviner is well suited to the majority of lunar compositions (as shown in its ability to define CF for the Apollo samples), the LTM CF will better characterize the composition of regions such as the highly silicic volcanic constructs identified in Glotch et al. (2010) and regions spectral dominated by olivine at VNIR wavelengths, such as those in Arnold et al. (2016), that were not easily distinguishable with the Diviner data.

After this analysis of methodology, the selective LTM channel fitting methods (Section 2.2.1 methods 3 and 4) produced the most accurate values and showed an improvement over the Diviner parabolic fitting for the range of samples in our spectral library. The maximum-value fit was chosen as the most consistent, and simplest implementation (Figure 6). However, as LTM has filters covering the same wavelengths as Diviner, we will also provide an LTM "Diviner" CF value, using methodology from Greenhagen et al. (2010) and described in Section 2.2.1 method 2 to allow comparisons between the data sets. While the LTM CF values and Diviner CF values will not provide the same value at some of the extreme compositional cases described above due to the limits of the Diviner wavelength range, much of the Moon's surface composition does have CF values within the overlapping range. Therefore, we will be able to provide this "heritage" parameter for use in direct comparisons between the data sets, particularly, as Diviner (and Lunar Reconnaissance Orbiter) have global coverage (at ~200 m/pixel resolution) compared to the targeted measurements LTM (and Lunar Trailblazer) will perform (at ~70 m/pixel resolution). These data sets combined will give us a greater understanding of what is identifiable at varied spatial scales.

4.2. Transparency Region

Both methods tested to classify this TF region short of the CF produce results giving the same overall trend as that seen in the laboratory resolution data. This similarity is unsurprising considering they are very similar methods,

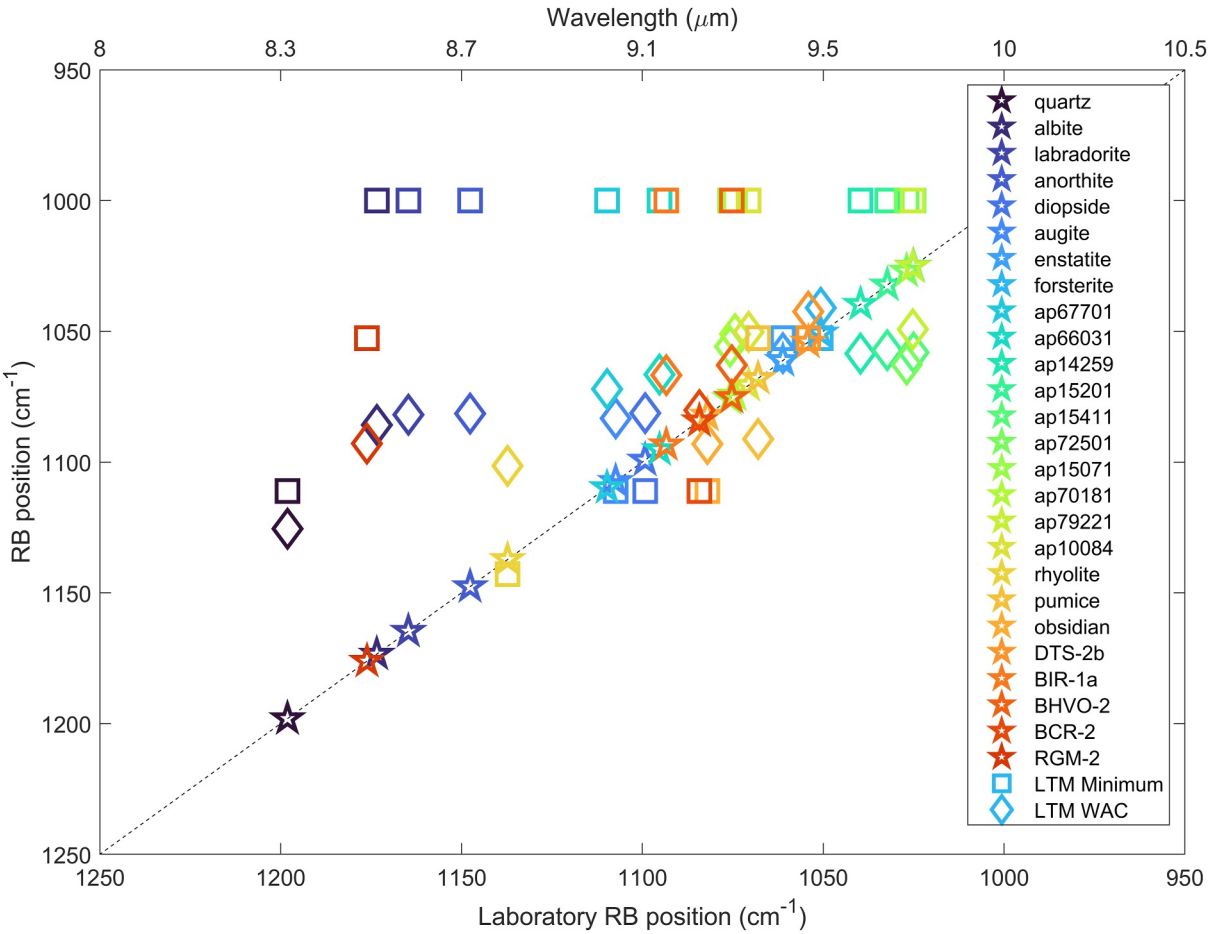

Figure 5. Comparison of the calculated Lunar Thermal Mapper RB position to the true values from the laboratory resolution data of the first RB minimum (stars).

with only the upper bound shifting. The values can have more variability, as there may be fewer data points over which to calculate slope, for example, more felsic compositions with very shortwave CFs will have limited coverage of the TF region. However, as both methods reflect the trends, we will use the true data points measured by LTM for this parameter (Section 2.2.2 method 2) to avoid over interpretation in the quick-look product and assign a NaN value if the c_{max} occurs at the 7 μm channel.

Our study also shows that the classification of this region will be more useful for intermediate to mafic compositions, where more of the region will be within the LTM wavelength range. Realistically, at the scale of LTM pixels, there will be a mix of regolith particle sizes and it is unlikely that an area on the order of 100s m^2 will be completely covered in <100 μm material, but this parameter may give us insight into particular areas of concentrated fines, or shed light on the contribution of fines to the overall spectrum (e.g., Edwards et al., 2018; Hayne et al., 2017). If not directly indicating particle size, this parameter can still highlight regions with interesting thermophysical properties for deeper analysis.

4.3. Reststrahlen Band Region

The RBs are difficult to capture with a single parameter, but the methods tested show a decent path to a quick-look product that can give an idea of the minimum in the RB region. The LTM WAC will not provide the center of a single RB, but for the total region captured within the LTM range (Figure 6). The LTM WAC gives a more useful, and dynamic value than simply using the location of the emissivity minimum, which is often just the value at the 10-μm channel.

We do observe a linear trend in the LTM WAC values but they have a lower slope than the laboratory values (Figure 5). The overall shift in position of the RBs with composition is similar to the CF trend, as the RBs are

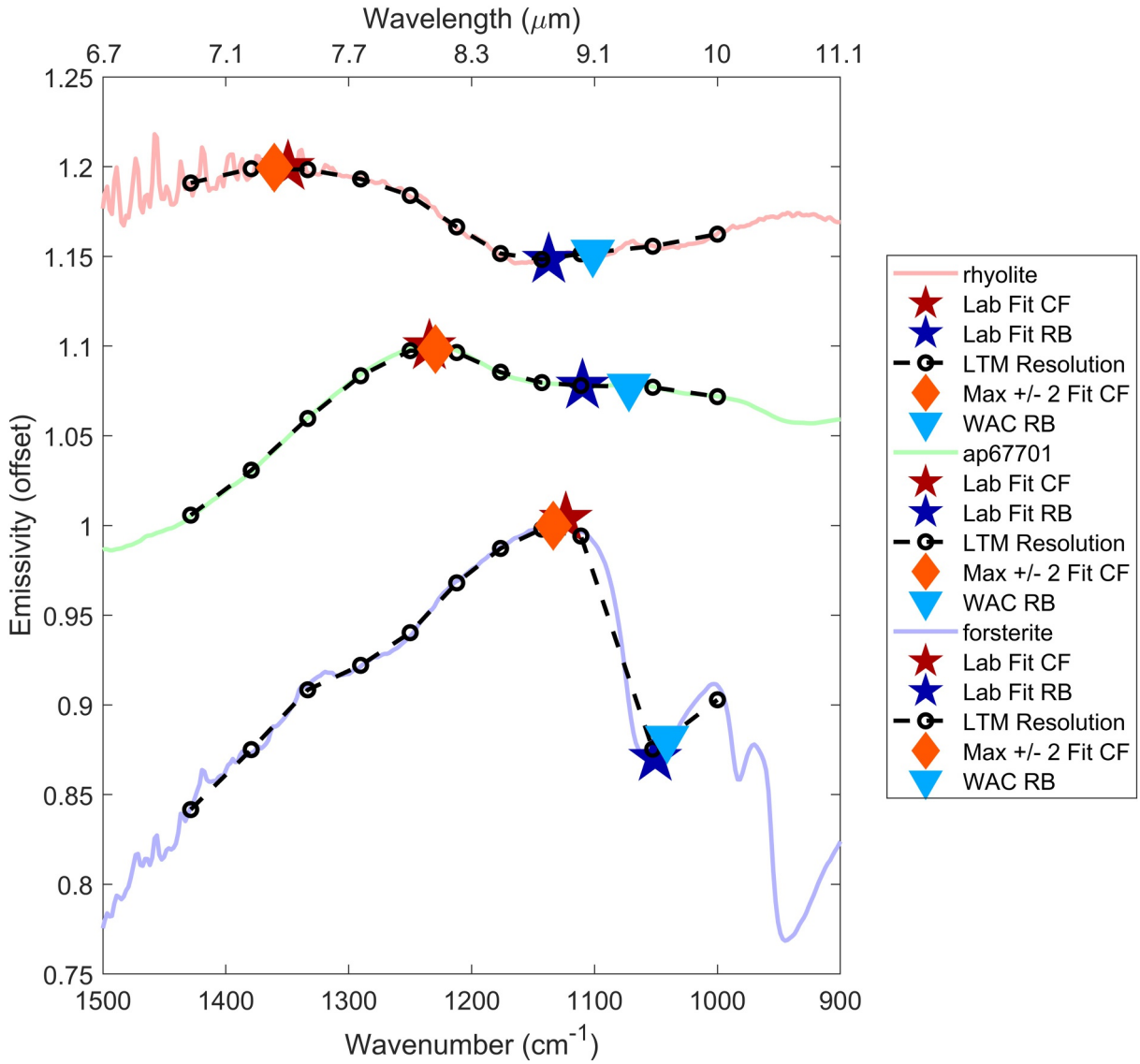

Figure 6. Examples of the best fit position parameter methods (diamond for the max-fit Christiansen feature (CF), triangle for weighted absorption center (WAC) RB) as compared to the laboratory values (stars, red for CF and blue for RB). The laboratory resolution spectra for rhyolite (pink), Apollo 67701 (green), and forsterite (purple) are shown overlaid with their Lunar Thermal Mapper resolution. As stated in 3.3, the WAC RB values are often at longer wavelengths than the first RB in the laboratory spectra.

located directly longward of the CF. The fact that this trend, though less pronounced, is still present in the LTM WAC values shows that this parameter is still a useful indicator of composition. A comparison of LTM CF value and LTM WAC values should therefore produce an idea of the overall composition, and a rough idea of the constituents. A more detailed look at the true LTM emissivity spectrum will be needed to better understand the composition.

5. Conclusions

These "quick-look" LTM mid-infrared parameters will provide a preliminary base for understanding and identifying compositions on the lunar surface. Based on this analysis, we have defined a final set of compositional parameters that we will use and provide to the scientific community. These final parameters and their methodology are summarized here:

1. **CF value** using the Max-Value polynomial fit (Section 2.2.1, method 4)

2. **WAC value** (Section 2.2.3, method 2)
3. **WAC band-depth** using 1- emissivity at LTM WAC value
4. **Transparency Roll-off** using the true LTM emissivity values (Section 2.2.2 method 2)
5. **Diviner Heritage CF value** parabolic fit to LTM's Diviner channels (Section 2.2.1 method 2)

These parameters should give us an easy way to identify areas of interest for both composition and physical properties that will then be compared with the parameters from HVM^3 (Dapremont et al., 2026) and further explored using the full range of data provided by Lunar Trailblazer.

Conflict of Interest

The authors declare no conflicts of interest relevant to this study.

Availability Statement

All laboratory spectra used in this work have been published in their cited works (Donaldson Hanna et al., 2017; Glotch et al., 2017; Shirley & Glotch, 2019) and the USGS terrestrial volcanic analogs spectra are available on Zenodo (Shirley, 2025).

Acknowledgments
The LTM instrument was supported by the UK Space Agency under their National Space Innovation, international bilateral, programme. The U.S. portions of the investigation were funded by NASA under contract to the Caltech campus (80MSFC19C0042) and to the Jet Propulsion Laboratory, California Institute of Technology (80NM0019F0079).

References

Amador, E. S., & Bandfield, J. L. (2016). Elevated bulk-silica exposures and evidence for multiple aqueous alteration episodes in Nili Fossae, Mars. *Icarus*, *276*, 39–51. https://doi.org/10.1016/j.icarus.2016.04.015

Arnold, J. A., Glotch, T. D., Lucey, P. G., Song, E., Thomas, I. R., Bowles, N. E., & Greenhagen, B. T. (2016). Constraints on olivine-rich rock types on the Moon as observed by Diviner and M3: Implications for the formation of the lunar crust. *Journal of Geophysical Research: Planets*, *121*(7), 1342–1361. https://doi.org/10.1002/2015je004874

Bowles, N. E., Ehlmann, B. L., Evans, R., Warren, T., Eshbaugh, H. H., King, G., et al. (2026). The Lunar Trailblazer Lunar Thermal Mapper. *Journal of Geophysical Research: Planets*. this issue. https://doi.org/10.1029/2025JE009333

Brown, E. C. (2023). *Exploring spectral unmixing algorithms for applications to estimating asteroid surface compositions*. Doctoral dissertation. University of Oxford. Retrieved from https://ora.ox.ac.uk/objects/uuid:ff0573d3-db31-4c80-9a82-d8c4feeb0dba

Conel, J. E. (1969). Infrared emissivities of silicates: Experimental results and a cloudy atmosphere model of spectral emission from condensed particulate mediums. *Journal of Geophysical Research*, *74*(6), 1614–1634. https://doi.org/10.1029/jb074i006p01614

Cooper, B. L., Salisbury, J. W., Killen, R. M., & Potter, A. E. (2002). Midinfrared spectral features of rocks and their powders. *Journal of Geophysical Research*, *107*(E4), 1-1–1-17. https://doi.org/10.1029/2000je001462

Dapremont, A. M., Klima, R. L., Wilk, K. A., Ehlmann, B. L., Edwards, C. S., Donaldson Hanna, K. L., et al. (2026). Visible-shortwave infrared (VSWIR) spectral parameters for the Lunar Trailblazer high-resolution volatiles and minerals Moon mapper (HVM^3). *Journal of Geophysical Research: Planets*. this issue. https://doi.org/10.1029/2025EA004557

Donaldson Hanna, K. D., Greenhagen, B. T., Patterson III, W. R., Pieters, C. M., Mustard, J. F., Bowles, N. E., et al. (2017). Effects of varying environmental conditions on emissivity spectra of bulk lunar soils: Application to Diviner thermal infrared observations of the Moon. *Icarus*, *283*, 326–342. https://doi.org/10.1016/j.icarus.2016.05.034

Donaldson Hanna, K. L., Bowles, N. E., Warren, T. J., Hamilton, V. E., Schrader, D. L., McCoy, T. J., et al. (2021). Spectral characterization of Bennu analogs using PASCALE: A new experimental set-up for simulating the near-surface conditions of airless bodies. *Journal of Geophysical Research: Planets*, *126*(2), e2020JE006624. https://doi.org/10.1029/2020je006624

Donaldson Hanna, K. L., Wyatt, M. B., Thomas, I. R., Bowles, N. E., Greenhagen, B. T., Maturilli, A., et al. (2012). Thermal infrared emissivity measurements under a simulated lunar environment: Application to the Diviner Lunar Radiometer Experiment. *Journal of Geophysical Research*, *117*(E12), E00H05. https://doi.org/10.1029/2011je003862

Edwards, C. S., Piqueux, S., Hamilton, V. E., Fergason, R. L., Herkenhoff, K. E., Vasavada, A. R., et al. (2018). The thermophysical properties of the Bagnold Dunes, Mars: Ground-truthing orbital data. *Journal of Geophysical Research: Planets*, *123*(5), 1307–1326. https://doi.org/10.1029/2017je005501

Ehlmann, B. L., Klima, R. L., Seybold, C. C., Klesh, A. T., Au, M. H., Bender, H. A., et al. (2022). NASA's Lunar Trailblazer mission: A pioneering small satellite for lunar water and lunar geology. In *2022 IEEE Aerospace Conference (AERO)* (pp. 1–14). IEEE.

Ehlmann, B. L., Klima, R. L., Seybold, C. C., Klesh, A. T., Bennett, C. L., & Bowles, N. (2026). The Lunar Trailblazer mission: Science motivation and implementation of a pioneering small satellite for lunar water and lunar geology in the NASA SIMPLEx program. *Earth and Space Science*. this issue. https://doi.org/10.1029/2025JE009300

Glotch, T. D., Lucey, P. G., Bandfield, J. L., Greenhagen, B. T., Thomas, I. R., Elphic, R. C., et al. (2010). Highly silicic compositions on the Moon. *Science*, *329*(5998), 1510–1513. https://doi.org/10.1126/science.1192148

Glotch, T. D., Shirley, K. A., & Greenhagen, B. T. (2017). Simulated lunar environment spectra of felsic rock particulates. In *48th Annual Lunar and Planetary Science Conference* (Vol. 1964, p. 1688).

Greenhagen, B. T., Lucey, P. G., Wyatt, M. B., Glotch, T. D., Allen, C. C., Arnold, J. A., et al. (2010). Global silicate mineralogy of the Moon from the Diviner Lunar Radiometer. *Science*, *329*(5998), 1507–1509. https://doi.org/10.1126/science.1192196

Hamilton, V. E., & Christensen, P. R. (2000). Determining the modal mineralogy of mafic and ultramafic igneous rocks using thermal emission spectroscopy. *Journal of Geophysical Research*, *105*(E4), 9717–9733. https://doi.org/10.1029/1999je001113

Hayne, P. O., Bandfield, J. L., Siegler, M. A., Vasavada, A. R., Ghent, R. R., Williams, J. P., et al. (2017). Global regolith thermophysical properties of the Moon from the Diviner Lunar Radiometer Experiment. *Journal of Geophysical Research: Planets*, *122*(12), 2371–2400. https://doi.org/10.1002/2017je005387

Henderson, B. G., & Jakosky, B. M. (1994). Near-surface thermal gradients and their effects on mid-infrared emission spectra of planetary surfaces. *Journal of Geophysical Research*, *99*(E9), 19063–19073. https://doi.org/10.1029/94je01861

Hunt, G. R., & Vincent, R. K. (1968). The behavior of spectral features in the infrared emission from particulate surfaces of various grain sizes. *Journal of Geophysical Research*, *73*(18), 6039–6046. https://doi.org/10.1029/jb073i018p06039

Logan, L. M., Hunt, G. R., Salisbury, J. W., & Balsamo, S. R. (1973). Compositional implications of Christiansen frequency maximums for infrared remote sensing applications. *Journal of Geophysical Research*, *78*(23), 4983–5003. https://doi.org/10.1029/jb078i023p04983

Lyon, R. J. P. (1964). Evaluation of infrared spectrophotometry for compositional analysis of lunar and planetary regoliths. Part II-rough and powdered surfaces (No. NASA-CR-100).

Mustard, J. F., & Hays, J. E. (1997). Effects of hyperfine particles on reflectance spectra from 0.3 to 25 μm. *Icarus*, *125*(1), 145–163. https://doi.org/10.1006/icar.1996.5583

Paige, D. A., Foote, M. C., Greenhagen, B. T., Schofield, J. T., Calcutt, S., Vasavada, A. R., et al. (2010). The lunar reconnaissance orbiter diviner lunar radiometer experiment. *Space Science Reviews*, *150*, 125–160. https://doi.org/10.1007/s11214-009-9529-2

Ruff, S. W., & Christensen, P. R. (2002). Bright and dark regions on Mars: Particle size and mineralogical characteristics based on Thermal Emission Spectrometer data. *Journal of Geophysical Research*, *107*(E12), 2-1–2-22. https://doi.org/10.1029/2001je001580

Salisbury, J. W., & Eastes, J. W. (1985). The effect of particle size and porosity on spectral contrast in the mid-infrared. *Icarus*, *64*(3), 586–588. https://doi.org/10.1016/0019-1035(85)90078-8

Salisbury, J. W., Vincent, R. K., Logan, L. M., & Hunt, G. R. (1970). Infrared emissivity of lunar surface features: 2. Interpretation. *Journal of Geophysical Research*, *75*(14), 2671–2682. https://doi.org/10.1029/jb075i014p02671

Salisbury, J. W., & Wald, A. (1992). The role of volume scattering in reducing spectral contrast of reststrahlen bands in spectra of powdered minerals. *Icarus*, *96*(1), 121–128. https://doi.org/10.1016/0019-1035(92)90009-v

Salisbury, J. W., Walter, L. S., & Vergo, N. (1987). *Mid-infrared (2.1–25 um) spectra of minerals* (No. 87-263). US Geological Survey.

Shirley, K. (2025). MIR spectra of terrestrial volcanic samples [Dataset]. *Zenodo*. https://doi.org/10.5281/zenodo.15806454

Shirley, K. A., & Glotch, T. D. (2019). Particle size effects on mid-infrared spectra of lunar analog minerals in a simulated lunar environment. *Journal of Geophysical Research: Planets*, *124*(4), 970–988. https://doi.org/10.1029/2018je005533

Smith, M. R., Bandfield, J. L., Cloutis, E. A., & Rice, M. S. (2013). Hydrated silica on Mars: Combined analysis with near-infrared and thermal-infrared spectroscopy. *Icarus*, *223*(2), 633–648. https://doi.org/10.1016/j.icarus.2013.01.024

Thompson, D. R., Green, R. O., Ehlmann, B. L., Klima, R., Pieters, C., Blaney, D., et al. (2025). Calibration and performance of the high resolution volatiles and minerals Moon mapper (HVM^3). *Journal of Geophysical Research: Planets*. https://doi.org/10.1029/2025EA004456

Vincent, R. K., & Thomson, F. (1972). Spectral compositional imaging of silicate rocks. *Journal of Geophysical Research*, *77*(14), 2465–2472. https://doi.org/10.1029/jb077i014p02465